

Original Article

A patient-enriched *MEIS1* coding variant causes a restless legs syndrome-like phenotype in mice

Chia-Luen Leu¹, Daniel D. Lam^{1,2}, Aaro V. Salminen^{1,2}, Benedikt Wefers³, Lore Becker⁴, Lillian Garrett^{3,4}, Jan Rozman^{4,5,6} , Wolfgang Wurst^{3,7,8,9}, Martin Hrabě de Angelis^{4,5,10}, Sabine M. Höltzer³ , Juliane Winkelmann^{1,2,9} and Rhiannon H. Williams^{1,*}

¹Institute of Neurogenomics, Helmholtz Center Munich, German Research Center for Environmental Health, Neuherberg, Germany

²Institute of Human Genetics, Klinikum rechts der Isar, School of Medicine, Technical University of Munich, Munich, Germany

³Institute of Developmental Genetics, Helmholtz Center Munich, German Research Center for Environmental Health, Neuherberg, Germany

⁴Institute of Experimental Genetics, German Mouse Clinic, Helmholtz Center Munich, Neuherberg, Germany

⁵German Center for Diabetes Research (DZD), Neuherberg, Germany

⁶Luxembourg Centre for Systems Biomedicine, University of Luxembourg, Belvaux, Luxembourg

⁷German Center for Neurodegenerative Diseases (DZNE), Site Munich, Germany

⁸Chair of Developmental Genetics, TUM School of Life Sciences, Technische Universität München, Freising, Germany

⁹Munich Cluster for Systems Neurology (SyNergy), Munich, Germany

¹⁰Chair of Experimental Genetics, TUM School of Life Sciences, Technische Universität, München, Freising, Germany

*Corresponding author. Rhiannon H. Williams, Email: rhiannon.williams@helmholtz-muenchen.de

Abstract

Restless legs syndrome (RLS) is a neurological disorder characterized by uncomfortable or unpleasant sensations in the legs during rest periods. To relieve these sensations, patients move their legs, causing sleep disruption. While the pathogenesis of RLS has yet to be resolved, there is a strong genetic association with the *MEIS1* gene. A missense variant in *MEIS1* is enriched sevenfold in people with RLS compared to non-affected individuals. We generated a mouse line carrying this mutation (p.Arg272His/c.815G>A), referred to herein as *Meis1*^{R272H/R272H} (*Meis1* point mutation), to determine whether it would phenotypically resemble RLS. As women are more prone to RLS, driven partly by an increased risk of developing RLS during pregnancy, we focused on female homozygous mice. We evaluated RLS-related outcomes, particularly sensorimotor behavior and sleep, in young and aged mice. Compared to noncarrier littermates, homozygous mice displayed very few differences. Significant hyperactivity occurred before the lights-on (rest) period in aged female mice, reflecting the age-dependent incidence of RLS. Sensory experiments involving tactile feedback (rotarod, wheel running, and hotplate) were only marginally different. Overall, RLS-like phenomena were not recapitulated except for the increased wake activity prior to rest. This is likely due to the focus on young mice. Nevertheless, the *Meis1*^{R272H} mouse line is a potentially useful RLS model, carrying a clinically relevant variant and showing an age-dependent phenotype.

Key words: *MEIS1*; restless legs syndrome; mouse model

Graphical Abstract



Created with Biorender.com

Submitted for publication: July 14, 2023; Revised: December 10, 2023

© The Author(s) 2024. Published by Oxford University Press on behalf of Sleep Research Society. All rights reserved. For commercial re-use, please contact reprints@oup.com for reprints and translation rights for reprints. All other permissions can be obtained through our RightsLink service via the Permissions link on the article page on our site—for further information please contact journals.permissions@oup.com.

Statement of Significance

RLS is a relatively prevalent neurological disorder with poorly understood pathophysiology. In this work, we generated a mouse model carrying a coding mutation in the *MEIS1* gene that is highly enriched in people with RLS. This back-translated mouse model showed classical signs of RLS, including hyperactivity near the start of the rest period and age dependence of phenotypes. This mouse model represents a potentially useful tool for further understanding RLS pathophysiology and bridging between mouse and human based on a precisely defined and disease-relevant variant.

Introduction

Restless legs syndrome (RLS) is a neurological disorder with the most common symptom being an urge to move and an unpleasant sensation felt in the legs at night [1]. This manifestation can occur during extended periods of rest, e.g. sitting quietly, and it is not directly correlated to sleep onset [2]. Therefore, RLS is attributed to a sensorimotor abnormality despite directly impacting sleep quality. The impact on sleep loss is reflected in patient complaints of daytime sleepiness, memory impairment, and depressed mood [3].

RLS has an estimated heritability of 50%–60% based on family and twin studies [4–8]. Epidemiological studies have suggested that the age-dependent prevalence of RLS is 2.5%–15% in European, American, and Australian populations [4, 6, 9, 10]. Symptoms generally progress with age [5], and women are more likely to be affected [11, 12]. A series of genome-wide association studies have provided insight into the complex genetic architecture. Several genes have been associated with RLS, including *MEIS1*, *BTBD9*, *MAP2K5*, *SKOR1*, and *PTPRD* [13, 14]. Among these genes, *MEIS1* consistently shows the strongest genetic association with RLS across studies [7, 14]. While the pathogenesis of RLS has yet to be determined, research consistently indicates a role for striatal dopaminergic dysfunction and iron deficiency [15, 16].

Dopaminergic medication can be effective in treating RLS but often becomes counterproductive due to paradoxical worsening of symptoms, a phenomenon known as augmentation [6]. Other treatment options are available, including GABA analogs and opioids, but successful long-term disease management is rare [9]. The development of more effective therapies is limited by a lack of understanding of the pathophysiology and a previous lack of consensus on RLS-like readouts in rodents [17].

MEIS1 encodes a homeodomain-containing transcription factor of the three amino acid loop extension superclass [16]. Due to the inferred importance of *MEIS1* in RLS, this gene has been targeted through animal models to delineate its role in RLS pathogenesis. Examples of rodent genetic models include mice heterozygous for *Meis1* null alleles, including *Meis1*^{tm1Mtor} [18, 19] and *Emx*^{Cre};*Meis1*^{fllox} mice [20]. Mice homozygous for *Meis1* null alleles demonstrate poor viability and have a variety of behavioral abnormalities, indicating that for functional studies, rodent models should preferably carry at least one intact allele. A phenotypic investigation found that both mouse lines had different RLS-like symptoms. Male *Meis1*^{tm1Mtor} mice were hyperactive while both sexes had a small deficit in auditory prepulse inhibition (PPI), the sensitivity of which was age-related [19]. In a subset of men with RLS, no ASR or PPI deficits were reported [21], highlighting the difficulty in matching rodent models to RLS features and the complexity of symptoms among patients. Sleep–wake assessment indicated *Meis1* heterozygous mice trended towards reduced delta power in EEG spectra [22], yet no significant changes in sleep structure were detected. These findings support the hypothesis that impairment of *Meis1* function affects sleep but does not directly cause

abnormalities in sleep circuitry. Male *Meis1* KO mice also were more active than noncarrier littermates, with increased likelihood of waking during the inactive phase, supporting an RLS-like phenotype [20]. Notably, both models indicate a large variability in effect size within carriers, adding to the complexity of resolving the contribution of *Meis1* to RLS circuitry.

Sequencing of *MEIS1* coding sequences in German with RLS (*n* = 3262) and controls (*n* = 2944) identified coding variants that were enriched in people with RLS, most notably p.Arg272His (R272H) which was observed approximately sevenfold more frequently in people with RLS than in population controls [8]. Given the prominent genetic association of the *MEIS1* locus with RLS, the precise mechanisms linking *MEIS1* to RLS pathogenesis are under intensive investigation. Regulation of forebrain development and iron homeostasis/metabolism has received particular attention [23]. As a lack of robust animal models hampers progress in developing improved treatments, we generated mice homozygous for the R272H missense mutation, identified as *Meis1*^{R272H} (*MEIS1* point mutation) mice, and characterized their phenotype. Since females are more prone to develop RLS, we focused on female mice.

Methods

Generation of *Meis1*R272H mice

Meis1^{R272H} mice were generated to include a point mutation at p.Arg272His (R272H) in *MEIS1* on a C57BL/6N background [24, 25]. C57BL/6N wild-type (WT) zygotes were microinjected with Cas9, a *Meis1*-specific sgRNA (protospacer AAAAAGCGTCACAAAAAGCG), and a single-stranded oligodeoxynucleotide as repair template for homology-directed repair. The oligonucleotide carried the intended R272H substitution as well as four silent mutations for genotyping purposes. The point mutation aimed at the nucleotide at position 815 within the gene *MEIS1*, and replaced nucleotide guanine by adenine. This resulted in the change of amino acid from arginine to histidine at position 272 in the *MEIS1* protein. A mutant founder animal was crossed to C57BL/6N WTs to establish the mouse line. Afterward, the line was maintained by crossing to WT C57BL/6J OlaHsd (Harlan) mice every 10 generations. Experimental cohorts were generated by breeding heterozygote × heterozygote carriers to obtain heterozygote (Het), homozygote (HOM), and non-carrier (WT) littermates. Genotypes were confirmed by sequencing targeted at position 815 within the gene *MEIS1*.

Mice for experiments

Mice were bred at Helmholtz Munich in accordance with EU regulations. Food (Altromin 1324, Lage, Germany) and water were provided *ad libitum*, with 12 h:12 h dark–light cycle (lights on 06:00 a.m. unless stated otherwise) and humidity 55 ± 10%. Female homozygote *Meis1*^{R272H/R272H} (*MEIS1* point mutation) and WT littermates were generated for the studies. Body weights of mice were

comparable between genotypes across age groups. In all recording environments, the bedding type used (wood shavings and paper tissue) and lighting conditions were maintained for consistency. Genotypes were tested randomly and the experimenter was blind to cohort identity.

Due to phenotyping pipelines, mice were split into three different cohorts for specific paradigms (Figure 1). The first cohort used 15 mice per genotype, 2–5 months of age and was examined by the standardized phenotyping analysis of the German Mouse Clinic including open field (distance traveled), indirect calorimetry (RER, respiratory exchange ratio), rotarod, and hot plate test behavioral responses [26, 27]. The second and third cohorts were designed to assess wheel running (WR) and activity patterns with aging ($n = 7\text{--}11/\text{genotype}$). The second cohort was young adults, 2–3 months of age for WR and 4–6 months of age for Piezo Sleep screen. The third cohort was older adults, 10–11 months for WR and 12–14 months for Piezo Sleep screen.

Open field test

The Open field test was carried out according to standardized phenotyping screens developed by the IMPC partners (<https://www.mousephenotype.org/impress/index>). The test apparatus (from ActiMot, TSE Systems, Berlin, Germany) is a square-shaped frame with two pairs of light-beam strips; each pair consisting of one transmitter strip and one receiver strip. The strips are arranged at right angles to each other in the same plane, permitting X and Y coordinate determination for animal location. Each strip has 16 infrared sensors, spaced 28 mm apart. The light barriers scan at 100 Hz frequency. If an even number of light beams are interrupted, the center of gravity is then calculated between adjacent sensors. Each test apparatus consists of a transparent and infrared light permeable acrylic test arena (internal measurements: $45.5 \times 45.5 \times 39.5$ cm) with a smooth floor. The illumination levels are set at ~150 lux in the corners and 200 lux in the middle of the test arena. Before each test period, mice were transported to the test room and left undisturbed for at least 30 min. Each mouse was placed individually into the middle of the arena facing the wall and allowed to explore freely for 20 min. The distance traveled was recorded during the test.

Wheel running

Mice were moved to individual home-cages that were equipped with wheels to permit voluntary WR activity. Running-wheel

activity was recorded for 3 weeks and the number of rotations was evaluated. Mice were removed from analyses if there was a failure to collect WR activity consistently during the experiment.

Indirect calorimetry

The determination of metabolic rate and substrate utilization, in combination with the monitoring of food and water uptake, and locomotor activity (equivalent to ActiMot) was based on indirect calorimetry [28]. High-precision CO_2 and O_2 sensors measure the difference in CO_2 and O_2 concentrations in air flowing through control and animal cages. Oxygen consumption and CO_2 production are calculated from differential gas concentrations and subtracted from air flow rates, and expressed as mL O_2 or $\text{CO}_2 \cdot \text{h}^{-1} \cdot \text{animal}^{-1}$. O_2 consumption and CO_2 production permit the calculation of the RER (VCO_2/VO_2), a surrogate measure for substrate utilization. An RER value ~0.7 indicates that fatty acids are the primary substrate for oxidative metabolism, while an RER ~1.0 indicates carbohydrate is the primary energy substrate [29, 30]. Each mouse was placed individually in the chamber for 21 h. Locomotor activity was measured as distance traveled.

Rotarod

The rotarod (Bioseb, Chaville, France) was used to measure forelimb and hindlimb motor coordination, balance, and motor learning ability [31]. External stimuli including noise and movement were minimized. The rotarod device is equipped with a computer-controlled motor-driven rotating rod, with five compartments to simultaneously test five mice. Magnetic sensors are used to detect when a mouse falls from the rotarod. In general, the mouse is placed perpendicular to the axis of rotation, with head facing the direction of the rotation. All mice were placed on the rotarod at an accelerating speed from 4 to 40 rpm for 300 s with 15 min between each trial. In motor coordination testing, mice were given three trials at the accelerating speed on one test day. The reason for the trial end (falling, jumping, or rotating passively) was recorded and used in subsequent analysis.

Hot plate

Mice were placed on a metal surface maintained at $52 \pm 0.2^\circ\text{C}$ (TSE GMBH, Germany; [32]). Locomotion of the mouse on the hot plate was constrained by a 20 cm high Plexiglas wall with a circular diameter area of 28 cm. Mice remained on the plate until they

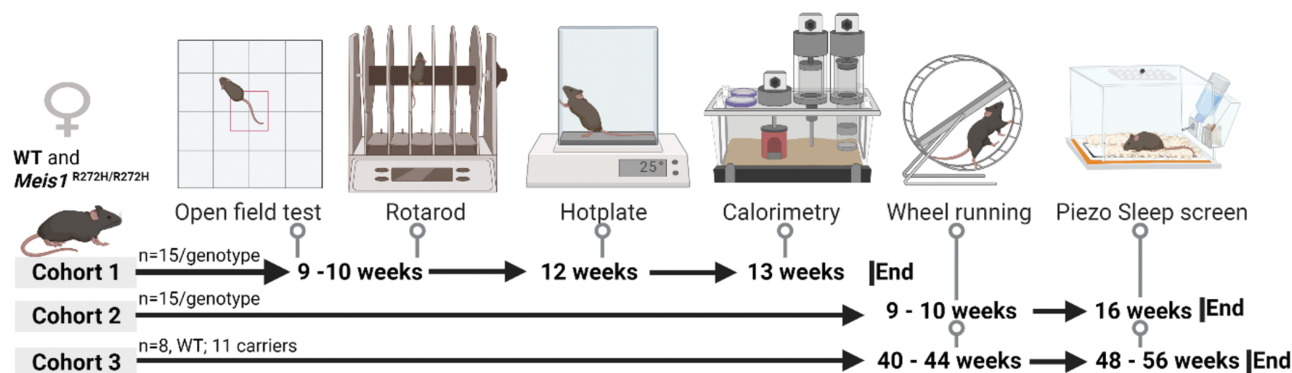


Figure 1. Summary of behavioral tests and timeline for each experimental cohort examined (created with BioRender.com).

performed one of three behaviors regarded as indicative of nociception: hind paw lick (licking), hind paw shake/flutter (shaking), or jumping. Only hind paw and not front paw responses were evaluated. This was to prevent false association of paw licking and lifting driven from normal grooming behavior with nociceptive processing. The latency was recorded to the nearest 0.1 s. To avoid tissue injury in each mouse, a maximum exposure time of 30 s was used.

Sleep screen

The sleep screen (Signal Solutions, LLC, Lexington, KY, USA) uses a specialized housing cage with a sensitive piezoelectric film mat placed on the floor of each cage. This film transforms mechanical pressure into electrical signals with a voltage that is proportional to the compressive mechanical strength. Using proprietary algorithms to detect breathing and gross locomotor activity, the sleep screen differentiates between sleep-like and waking activity of the mouse [33]. Piezo signals were acquired with the MouseRec acquisition system (Signal Solutions, LLC). Output signals were amplified and filtered between 0.5 and 10 Hz. The amplified signals were analog-to-digital (A/D) converted at a sampling rate of 128 Hz using the LabView 7.1 software (National Instruments, Austin, TX, USA). Piezo signals were analyzed over tapered 8-s windows at a 2-s increment, from which a “decision statistic” was computed [33]. Each mouse was placed individually in a piezo cage for a period of 72 h. The first 24 h were used as an acclimatization period. All signals were acquired and analyzed with SleepStats Data Explorer (v2.181, Signal Solutions, LLC, 2020). State transitions and the average sleep and wake bout duration in different time bins were assessed from the 2-day recording period post acclimatization. Dawn was calculated at ZT 23–1 and dusk at ZT 11–13. The breathing rate assessment was computed only in periods of sleep, as the algorithm cannot detect the changes in thorax pressure required with sufficient sensitivity when any locomotion is present.

Clinical chemistry

The screen was performed using a Beckman-Coulter AU 480 auto-analyzer and adapted reagents from Beckman-Coulter (Krefeld, Germany), except free fatty acids (Non-esterified fatty acid, NEFA) that were measured using a kit from Wako Chemicals GmbH (NEFA-HR2, Wako Chemicals, Neuss, Germany) and Glycerol, which was measured using a kit from Randox Laboratories GmbH (Krefeld, Germany). In the primary screen, a broad set of parameters was measured including various enzyme activities, as well as plasma concentrations of specific substrates and electrolytes in young (12 weeks old) ad libitum fed mice [31, 34] ($n = 15/\text{genotype}$). There were no phenotypic quality differences in any of the measures. Here reported is plasma concentration of the following electrolytes: calcium, inorganic phosphate, iron; as well as unsaturated iron binding capacity (UIBC), calculated: total iron binding capacity from iron plus UIBC (TIBC—surrogate marker for transferrin), transferrin saturation as proportion % of iron of TIBC.

Statistics

Statistical analyses were performed in R (R Foundation for Statistical Computing, v4.1.1). Before statistical analyses, we

confirmed the normality of variance to confirm equal population distributions. Genotype effects in distance traveled, WR, indirect calorimetry, and hot plate test were examined by applying unpaired Student's t-test after confirming equal population distribution. A Wilcoxon rank sum test (Mann-Whitney U-test) was used to examine genotype effects in rotarod and piezo Sleep screen recording due to unequal population distribution. Statistical significance was set to $p < .05$. Pearson correlation tests were performed to quantify the correspondence between different phenotypes. Regression analyses were run on R to visualize the distribution of phenotypes. Principal component analysis (PCA) and uniform manifold approximation and projection (UMAP) were both performed to reduce the dimensionality of phenotypic datasets and increase the interpretability but at the same time, minimizing information loss. PCA and UMAP were performed based on six phenotypic results: hot plate reaction time, distance traveled, falling proportion from the rotarod, time spent in center, RER (VCO_2/VO_2) in light period, and RER (VCO_2/VO_2) in dark period. PCA and UMAP were run on R.

Results

The generation of *Meis1*^{R272H} mice, both heterozygous and homozygous, produced viable offspring with expected genotype proportions (Supplementary Table S1). No indications that the point mutation affected mouse health or welfare, or caused abnormal phenotypic impacts in either sex were observed.

Lack of gross motor function changes in *Meis1*^{R272H/R272H} mice

To evaluate the *Meis1*^{R272H/R272H} mouse as a potential model for RLS, we focused on phenotypic assays of sensorimotor function. When housed with running wheels, young *Meis1*^{R272H/R272H} mice ran 784 ± 85 rev compared to age-matched WT (1064 ± 147 rev; $n = 7/\text{genotype}$; $p\text{-value} = .46$) in 24 h. When activity during light (inactive) and dark (active) periods was assessed separately, the revolutions were *Meis1*^{R272H/R272H} L: 60 ± 7 , D: 1508 ± 167 ; WT L: 70 ± 9 , D: 2058 ± 288 rev ($p\text{-value} > .9$ and $.02$, respectively). The aged cohorts ran less in the same analysis period. Aged *Meis1*^{R272H/R272H} mice ($n = 9$) ran 566.2 ± 94.4 rev compared to age-matched WT (468.6 ± 92.5 rev; $n = 6$; $p\text{-value} = .95$) in 24 h. When activity during light and dark periods was assessed separately, the revolutions were *Meis1*^{R272H/R272H} L: 53.8 ± 9.2 , D: 1078.6 ± 181.4 ; WT L: 29.9 ± 6.7 , D: 907.4 ± 179.1 ($p\text{-value} = .99$ and $.8$, respectively). Overall, *Meis1*^{R272H/R272H} mice did not show the typical hyperactivity in the active period observed in other RLS mouse models (Figure 2, A and B; Supplementary Table S2A).

Indirect calorimetry ($n = 15/\text{genotype}$) was performed for 21 h. During the light period (9 h) *Meis1*^{R272H/R272H} RER averaged 0.85 ± 0.01 and WT 0.82 ± 0.01 ($p\text{-value} > .9$). In the dark phase (12 h), these values were 0.87 ± 0.02 and 0.84 ± 0.01 ($p\text{-value} = .85$), respectively. There were no statistically significant differences between genotypes at any time phase examined for RER nor in activity (Figure 2, C–F; Supplementary Table S2B).

In the open field test, *Meis1*^{R272H/R272H} mice ($n = 15$) traveled an average distance of 20.30 m, compared to 18.14 m for the WT littermates ($n = 15$) in the 20 min period assessed ($p\text{-value} = .12$, Figure 2, G). *Meis1*^{R272H/R272H} mice spent more time in the center at 10 min (32% vs. 20% for WT; $p\text{-value} = .11$) but overall did not differ significantly from WT in any parameter measured in the open field test (including rearing, speed, or resting time).

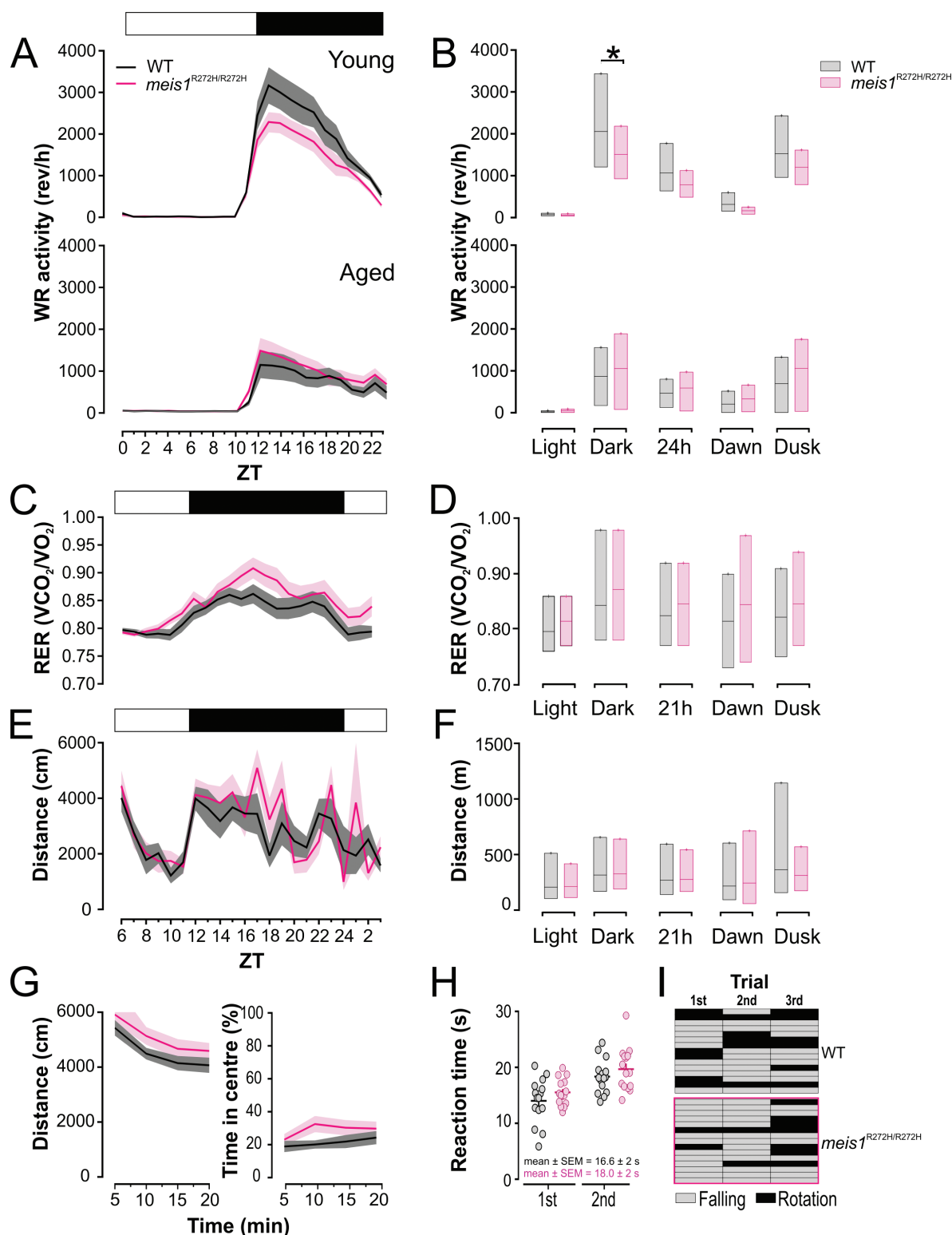


Figure 2. Locomotor activity, calorimetry, and sensory responses in *Meis1*^{R272H/R272H} mice. (A, B) Wheel-running (WR) activity across 24 h in young (top) and aged (bottom) *Meis1*^{R272H/R272H} and WT mice. Summary of WR characteristics across different analysis periods relative to age and genotype. Dawn (ZT 23–1) and dusk (ZT 11–13) were also measured. There was a significant difference between WR activity during the dark phase in young mice, with more activity in WT (**p* = .04; 2-way RM-ANOVA). Line: mean ± SEM. (C, D) RER (VCO₂/VO₂) in indirect calorimetry across 21 h sampling. *Meis1*^{R272H/R272H} mice demonstrated increased RER during the dark period but this did not reach significance. Summary of RER characteristics between genotypes. (E, F) Locomotor activity of mice during calorimetry measurements. There was no evidence for different locomotor patterns between the different genotypes. (G) Locomotor activity in the open field. *Meis1*^{R272H/R272H} mice were more active compared to WT and spent more time in the center. The differences did not reach statistical significance. (H) Hotplate sensory response was measured by reaction time in WT and *Meis1*^{R272H/R272H} mice. There was no significant difference between genotypes in trials. (I) Rotarod responses were compared between the proportion that fell and those that remained for the duration of the test. Despite *Meis1*^{R272H/R272H} mice tending to display a higher proportion of falling from the rotarod, no statistically significant effects compared to WT mice were reached (*p* = .33, Wilcoxon rank sum test).

Sensorimotor assessment

In the hot plate response test ($n = 15/\text{genotype}$), average reaction time across two trials for $\text{Meis1}^{\text{R272H/R272H}}$ mice was 18 ± 2.1 s, compared to 16.5 ± 2.2 s for WT littermates ($p\text{-value} = .18$; Figure 2, H). The first response type was predominately hind paw shaking (6/15 WT and 12/15 $\text{Meis1}^{\text{R272H/R272H}}$) while the second predominant response was hind paw licking (9/15 WT and 11/15 $\text{Meis1}^{\text{R272H/R272H}}$) for both genotypes.

$\text{Meis1}^{\text{R272H/R272H}}$ mice on the rotarod fell off on 75.6% of trials across all speeds tested, while WT fell off on 64% of trials ($n = 15/\text{genotype}$). The proportion of mice that remained on the rotarod for the duration of the test was similar between genotypes. While the respective distributions suggest a tendency for $\text{Meis1}^{\text{R272H/R272H}}$ mice to fall more often (Figure 2, I: 8 vs. 5 WT in first trial), there was no statistically significant difference between the genotypes.

No detectable differences in clinical chemistry in ad libitum fed mice

It is suggested that there may be a common genetic predisposition to RLS and iron deficiency also involving *MEIS1* [15]. Therefore, a clinical chemistry panel was carried out in 12-week-old female WT ($n = 15$) and $\text{Meis1}^{\text{R272H/R272H}}$ ($n = 15$) mice. There were no phenotypic differences in plasma concentrations of minerals, iron, and alkaline phosphatase (ALP) activity between young WT and $\text{Meis1}^{\text{R272H/R272H}}$ mice (Supplementary Table S3).

Sleep–wake activity is altered in $\text{Meis1}^{\text{R272H/R272H}}$ mice

Since sleep disturbance is a common symptom in people with RLS [35, 36], we determined whether the $\text{Meis1}^{\text{R272H/R272H}}$ mice recapitulate this phenotype. In young ($n = 10$) and aged ($n = 11$) $\text{Meis1}^{\text{R272H/R272H}}$ mice, the average wake time across 24 h compared to age-matched noncarriers showed comparable profiles (Figure 3, A). When collapsed as an average wake activity in 24 h with respect to age, this was 65.6 ± 4.9 % in young and 63.3 ± 3.9 % for aged $\text{Meis1}^{\text{R272H/R272H}}$; and 62 ± 4.7 % in young ($n = 10$) and 60.5 ± 3.7 % for aged ($n = 8$) WT mice (Figure 3, B). There were no differences in percent wake time in light or dark periods between ages or genotypes (all $p\text{-value} > .9$). Next, we assessed activity at dawn (ZT 23–1) and dusk (ZT 11–13), as RLS-like motor symptoms predominate at the rest transition in patients. $\text{Meis1}^{\text{R272H/R272H}}$ mice spent 91.3 ± 3.8 % (young) and 83.6 ± 2.9 % (aged) awake at dawn, while age-matched WT spent 81.8 ± 3.8 % and 72.43 ± 4 % in wake, respectively. These differences were statistically significant between genotypes for the aged cohort ($p = .029$; Supplementary Table S4A). For dusk, there were no significant differences between any of the tested groups (all $p\text{-value} > .9$). The wake bout durations for young and aged $\text{Meis1}^{\text{R272H/R272H}}$ mice also increased at the dawn transition but were not significantly different from age-matched WT (young WT: 17.7 ± 2.35 min, young $\text{Meis1}^{\text{R272H/R272H}}$: 26.78 ± 5.32 min, $p\text{-value} = .16$; aged WT: 17.66 ± 5.28 min, aged $\text{Meis1}^{\text{R272H/R272H}}$: 23.16 ± 4.71 min, $p\text{-value} = .7$).

Next, we assessed the number of state transitions across both ages with respect to genotype and time periods of interest. There were more state transitions in the light period, which increased with age, but which were not statistically significantly different between genotypes (young WT: 93.1 ± 8.5 , young $\text{Meis1}^{\text{R272H/R272H}}$: 87.2 ± 7.5 , $p\text{-value} > .9$; aged WT: 123.6 ± 6.3 , aged $\text{Meis1}^{\text{R272H/R272H}}$: 101.4 ± 6.6 , $p\text{-value} = .12$; Supplementary Table S4B). In the dark period, due to consolidation of wake, the number of transitions decreased but were again comparable between genotypes (young

WT: 62.4 ± 12.2 , young $\text{Meis1}^{\text{R272H/R272H}}$: 46.9 ± 7.55 , $p\text{-value} > .9$; aged WT: 70.4 ± 8.4 , aged $\text{Meis1}^{\text{R272H/R272H}}$: 59.4 ± 4.9 , $p\text{-value} > .9$). Over 24 h, the number of state transitions was not significantly different in young mice (WT: 157.5 ± 18.5 , $\text{Meis1}^{\text{R272H/R272H}}$: 136.1 ± 12.9 , $p\text{-value} = .54$) but was statistically significantly different in aged mice (WT: 196 ± 14.7 , $\text{Meis1}^{\text{R272H/R272H}}$: 162.8 ± 9.9 , $p\text{-value} = .005$), whereby $\text{Meis1}^{\text{R272H/R272H}}$ had less transitions.

To assess if the change in state transitions may be governed by fluctuation of one state, we also calculated the sleep or wake bout length average before a transition. Aged $\text{Meis1}^{\text{R272H/R272H}}$ mice had significantly longer sleep bout lengths in the light period (aged WT: 6.94 ± 0.35 min, aged $\text{Meis1}^{\text{R272H/R272H}}$: 8.84 ± 0.39 min, $p\text{-value} = .02$), which reduced to comparable bout length average at the dawn transition point. These effects were not seen in young mice (young WT: 10.95 ± 1.05 min, young $\text{Meis1}^{\text{R272H/R272H}}$: 10.13 ± 1.19 min, $p\text{-value} > .9$). Overall, there were more observable differences in aged mice, which for both genotypes are an increased consolidation of sleep time in the light period, and comparable wake bout length. There are significantly less transitions in female $\text{Meis1}^{\text{R272H/R272H}}$. At dawn, wake bout length increases and sleep time decreases in both genotypes; yet $\text{Meis1}^{\text{R272H/R272H}}$ have slightly longer wake bouts, reduced transitions, and reduced sleep time, resulting in significantly higher total percent wake activity.

Breathing rate in sleep is comparable between $\text{Meis1}^{\text{R272H/R272H}}$ and WT mice

The piezo sleep screen can determine the breathing rate during sleep periods. Breathing rates are an independent measure of arousal levels and sympathetic activity. Across 24 h, $\text{Meis1}^{\text{R272H/R272H}}$ mice had a breathing frequency of either 2.98 ± 0.07 Hz (young) or 3.10 ± 0.07 Hz (aged) which was comparable to age-matched WT littermates, 3.0 ± 0.05 Hz (young, $p\text{-value} > .9$) and 2.98 ± 0.08 Hz (aged, $p\text{-value} > .9$; Figure 3, D; Supplementary Table S5). There was no significant difference at any time period, including dusk and dawn, between genotypes. In addition, we assessed the periods where the breathing rate was lower than one-third of the average value in each time period which may be indicative of potential apneic events in sleep periods [31]. No significant differences were observed between genotypes, although the number (s/h) was higher in young mice compared to aged mice; and aged $\text{Meis1}^{\text{R272H/R272H}}$ had slightly more episodes (Supplementary Table S5).

Integration of phenotypic signatures for RLS-like mouse model

To determine if there was any commonality between phenotypic responses in locomotor assays and sensorimotor tasks, we computed Pearson correlation coefficients between traits and genotypes. Due to different experimental cohorts used across assays, we compared only those where more than one measure was available for the same individual mouse. Regression analysis failed to reach any significant differences between the two genotypes in most parameters examined. There was a significant negative correlation between hot plate response latencies and distance traveled, as measured in the calorimetry chamber for WT mice ($r = -0.51$, $p = .04$) that was absent in $\text{Meis1}^{\text{R272H/R272H}}$ ($r = -0.01$, $p = .94$; Figure 4, A).

In this study, multiple phenotypes were assessed, including WR activity, open field test, hot plate reaction time, rotarod, and sleep. Collectively, these measurements constitute a multidimensional composite phenotype of each mouse. We asked whether WT and

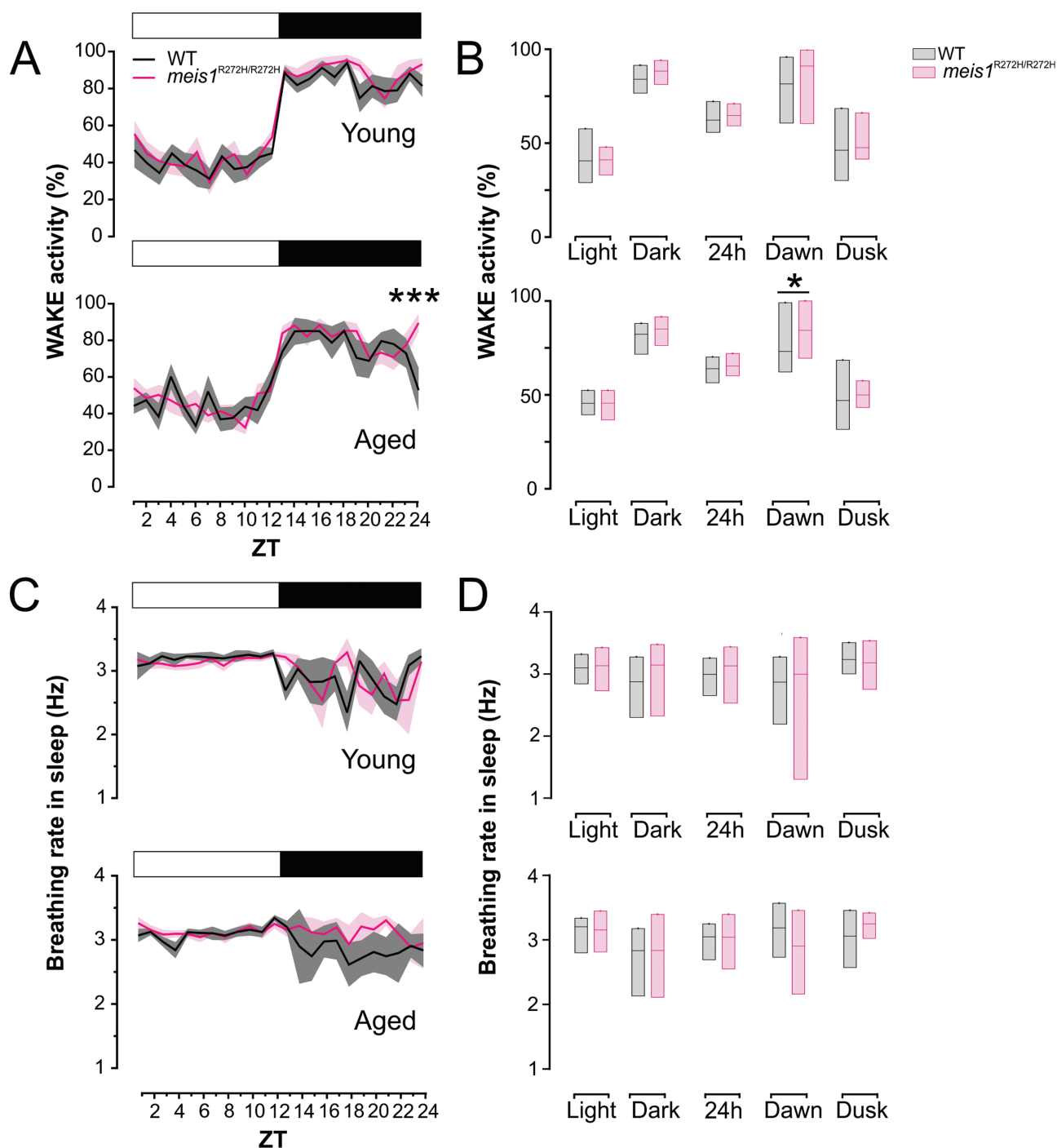


Figure 3. Piezo Sleep screen of wake activity and breathing rates. (A, B) Time spent in wake activity in young and aged *Meis1*^{R272H/R272H} and WT mice. There was a significant increase in wake activity in aged *Meis1*^{R272H/R272H} during the dawn transition (ZT23-1) period ($p = .029$, 2-way RM-ANOVA). The main response was driven by elevated activity at ZT23 ($p = .0009$). The other time periods examined did not show any significant difference. (C, D) Breathing rhythm (Hz) during sleep periods across 24 h. There were no significant differences in breathing activity between genotypes.

Meis1^{R272H/R272H} mice could be distinguished in their composite phenotypes, analogous to the approach used in Xie et al. [37].

To this end, we reduced the dimensionality of the composite phenotypes using a linear method, PCA, and a nonlinear method, UMAP. We extracted PCA loadings and UMAP embeddings for the composite phenotypes. Both the PCA and the UMAP methods suggested a subtle difference between genotypes. In the first principal component, which accounted for 37.9% of the variance, *Meis1*^{R272H/R272H} mice had higher loadings ($n = 11$ of 15, 0.55 ± 0.11)

than WT ($n = 11$ of 15, -0.550 ± 0.07 ; Figure 4, B and C). These loadings were significantly different between genotypes ($p = .045$). The third principal component (Figure 4, B, right panel) accounted for 17.4% of the variance, with *Meis1*^{R272H/R272H} mice having higher loadings ($n = 11$ of 15, 0.250 ± 0.06) than WT ($n = 10$ of 15, -0.250 ± 0.06 ; Figure 4, K). Thus, integrating phenotypes reveals an overall phenotypic shift in HOM mice. The UMAP (not shown) showed similar results, with a separation between *Meis1*^{R272H/R272H} mice and WT mice.

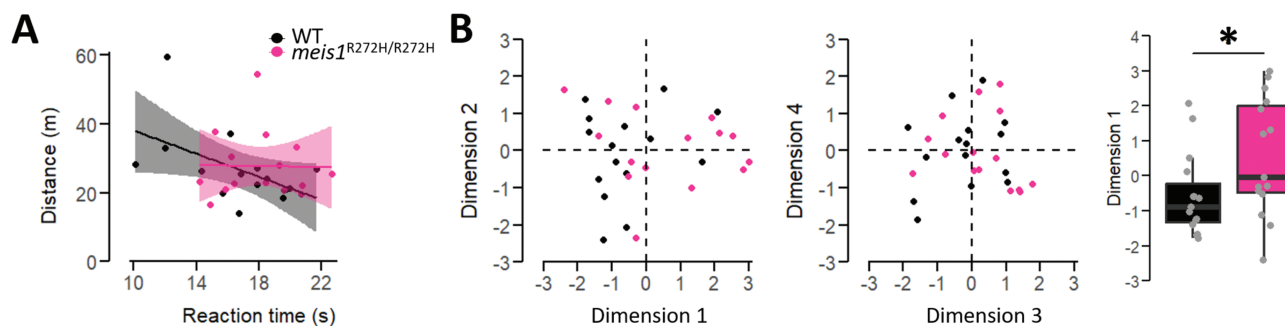


Figure 4. Integration of phenotypic signatures for RLS-like mouse model. (A) Regression correlation between reaction time in hot plate test and distance traveled in indirect calorimetry. WT mice had a negative correlation ($r = -0.51$, $p = .04$), while the correlation in *Meis1*^{R272H/R272H} mice was absent ($r = -0.01$, $p = .94$). (B, C) PCA between *Meis1*^{R272H/R272H} and WT mice based on main phenotypic signatures (Figure 2). Dimensions 1 summarized the greatest variation, a small yet significant difference, between the two genotypes in the respective parameters ($p = .045$).

Discussion

The aim of this study was to generate a mouse model based on a discrete missense variant within the *MEIS1* gene that is highly enriched in people with RLS. This represents a highly clinically relevant approach to understand RLS pathogenesis and permits recognition of phenotypes that may more closely represent clinical RLS, as opposed to more extreme and less specific phenotypes observed with *Meis1* null alleles. Despite the absence of homozygous carriers in the original cohort [24] and in gnomAD (out of 279 234 alleles), likely due to the low variant frequency of 0.02%, we chose to focus on homozygote female mice in the expectation that any presenting phenotype will be more pronounced, thereby aiding detection of specific disease features.

While male and female mice were both viable as heterozygote or homozygote carriers of the R272H mutation, we report the analyses of only the phenotypic features of female homozygote carriers and noncarrier littermates. This is due to the increased prevalence of RLS in females, which we believed might be replicated in the female cohorts. There was no effect of this mutation on development, exemplified by comparable weight gain, breeding viability, and behavioral attributes, e.g. no seizures or abnormal behavior, when compared to noncarriers. Therefore, we focused on phenotypes related to locomotion, balance, sensory processing, and sleep behaviors due to the prevalence of such symptoms in people with RLS. People with RLS generally present with restlessness or frequent arousals during rest periods, particularly before bedtime, due to an urge to move the legs [38]. Because this symptom is generalized across RLS, we focused on analyzing activity patterns around the transition to the rest period in the *Meis1*^{R272H/R272H} mice, in accordance with recommended consensus guidelines [17].

In the locomotor assays examined, *Meis1*^{R272H/R272H} mice demonstrated mixed responses compared to age-matched noncarriers. In WR, younger WT mice ran more than their female *Meis1*^{R272H/R272H} littermates, but this effect was lost in the aged cohort. In contrast, with age, the *Meis1*^{R272H/R272H} mice were hyperactive at the wake-sleep transition (dawn), recapitulating the core presentation in people with RLS [17]. The magnitude of the response was dependent on the particular behavioral assay, and the majority were assessed only in young mice. The sensory component of engaging in a running wheel may hinder the *Meis1*^{R272H/R272H} mice, whereas the piezo sleep-wake screen relies on home-cage monitoring. RLS incidence increases with age [17], most diagnoses occurring after 30 years of age in women [5, 37]. This may be a reason why there are almost no changes in locomotion in most

of the phenotypic tests, as most were performed in young adult mice (9–16 weeks of age). In aged females, the hyperactivity at dawn in *Meis1*^{R272H/R272H} mice is in accordance with a key feature commonly reported in RLS animal models e.g. *Meis1* null heterozygous mice are hyperactive in the open field test [21, 39], and *Btd9* mutant mice have elevated WR activity, albeit during the active period [36]. Notably, the timing of behavioral differences mainly occurs during the initial engagement of locomotion or at the end of a long bout of activity.

Apart from hyperactivity, there are also some indications of altered sensory feedback in RLS. For example, some people with RLS showed impaired balance and sensory functions, with RLS linked to an increased risk of falling in the elderly population (OR = 3.1, $p = .049$) [40] as well as an impairment of temperature perception [41]. When assessing sensorimotor function in the *Meis1*^{R272H/R272H} mice, the results were suggestive yet subtle, often failing to reach a statistical significance. Female *Meis1*^{R272H/R272H} did not demonstrate significant altered thermal sensitivity, similar to *Meis1* deficient mice [19], which may indicate that *MEIS1*-related RLS does not involve thermal hyperalgesia. This contrasts to the *Btd9* KO mouse, another RLS-like model, which had a dopamine-sensitive, circadian-dependent increase in thermal sensitivity measured by tail flick [36]. Bachman et al. [42] reported that C-fiber-mediated hypoalgesia occurs in patients with secondary RLS, whereby those with primary RLS only show differences in mechanical sensitivity. Follow-up studies with fiber-selective assessments would differentiate whether this mouse model has impaired descending inhibition or increased spinal excitability, which would better align it with symptoms in people with RLS.

Significant differences in sensorimotor and gross locomotor activity between WT and *Meis1*^{R272H/R272H} mice were not observed. However, responses in hot plate and locomotor behavior were correlated in WT but not in *Meis1*^{R272H/R272H}. By integrating all the phenotypic parameters, a significant difference between the genotypes was found in dimension 1 of the PCA. Overall, there was more phenotypic variance within the carrier cohort, possibly indicative of differential penetrance of the *Meis1*^{R272H} mutation. This is comparable to reported variation in patient symptoms and responses to sensory stimuli, e.g. differences in how patients experience temperature [43] or describe pain sensation [44], underlying the complex pathogenesis of RLS [38, 44]. The functional impact of the *Meis1*^{R272H} point mutation may be more subtle than that of a null allele, resulting in weaker phenotypes for some measures.

The piezo sleep-wake screen on a separate mouse cohort indicated a predominant increase in wake activity at dark-light

transition in female *Meis1*^{R272H/R272H} mice. As the piezo sleep screen determines wake activity by integrating gross locomotor activity with sensitive breathing measures, achieving an accuracy of 80%–90% compared to quantitative EEG [33], it is clear that this value is not driven by movement alone but reflects an increased arousal state. Whether this increased arousal is driven by uncomfortable sensations in the hindlimbs of the mice, similar to patients, is unclear—we could not separate specific hindlimb movement at rest from general grooming or twitching behavior in this experimental paradigm. Nevertheless, we observed a significant decrease in state transitions over 24 h in aged *Meis1*^{R272H/R272H} mice compared to aged WT. This suggests an altered arousal state and also implies that any RLS-like periodic leg movements were either not generated in this mouse line or not detectable via the piezo system. Contrary to our hypothesis, aged *Meis1*^{R272H/R272H} mice also had longer sleep bout durations in the light phase yet displayed more consolidated wake bouts at dawn. This latter effect, coupled with reduced state transitions led to the significantly increased wake time at dawn observed compared to aged WT.

We did not find changes in ad libitum fed plasma measures of iron or iron-related processes in the young female *Meis1*^{R272H/R272H} mice compared to WT. This would be of interest to investigate further, perhaps focusing on more aged cohorts and brain iron concentration. In addition, an iron challenge, such as a low-iron diet may be required to exacerbate the *Meis1*^{R272H/R272H} phenotype. A recent study observed that an iron-deficient diet induced an RLS-like mouse phenotype, depicted by altered spinal cord reflex excitability and reduced sleep time, and which was more prominent in females than males [45]. These responses were reversible when iron was reintroduced to the diet, also fitting with the observation that in two-thirds of patients who present with RLS in pregnancy, RLS symptoms disappear after delivery [46]. This experimental paradigm would be of particular interest to test on female *Meis1*^{R272H/R272H} mice.

Overall, we demonstrate that female *Meis1*^{R272H/R272H} mice are viable and have no physical disabilities. The main detectable RLS-like feature was hyperactivity at wake–rest transition in aged mice. Most other behavioral features are subtle and are not statistically significantly different from noncarriers, but when classed together, suggest a neural circuit reorganization. This supports the notion that RLS may not be caused by dysfunction in a single neural circuit, but that a pervasive developmental role of *MEIS1* drives a broad reorganization which predisposes to certain characteristics presenting as a range of symptom severity. Notably, increased locomotion and arousal state are the most consistent across RLS animal models. The data presented herein reflect the value of developing back-translated models to investigate human diseases in order to better understand their pathogenesis and heterogeneity. People with RLS having the *R272H* mutation represent only a small proportion of carriers, and specific RLS phenomena in these patients cannot be thoroughly investigated due to recruitment and identification sensitivity. Nevertheless, the *Meis1*^{R272H/R272H} mouse model represents a clinically relevant and phenotypically validated tool for gaining deeper understanding of RLS pathogenesis.

Supplementary Material

Supplementary material is available at *SLEEP* online. All data available upon request.

Acknowledgments

The authors thank the technical assistants in the Institute of Neurogenomics who contributed to mouse breeding and genotyping, and members of the German Mouse Clinic and Helmholtz Abteilung für Vergleichende Medizin staff for technical support.

Author Contributions

BW, WW, and JW generated the mouse line; AS, LG, LB, SH, JR, and MHdA conducted experiments; CCL, RHW, and DL analyzed the data and wrote the manuscript. RHW, MHdA, and JW provided financial support for the research.

Funding

This study was supported by internal funding (Helmholtz Munich) to JW; German Federal Ministry of Education and Research (Infrafrontier grant 01KX1012) and German Center for Diabetes Research (DZD) to MHdA; and by the ERC under the European Union's Horizon 2020 Research and Innovation Program Grant Agreement No. 715933 to RHW.

References

- Ekblom KA. Restless legs syndrome. *Neurology*. 1960;**10**:868–873. doi:[10.1212/wnl.10.9.868](https://doi.org/10.1212/wnl.10.9.868)
- Walters AS. Toward a better definition of the restless legs syndrome. The International Restless Legs Syndrome Study Group. *Mov Disord*. 1995;**10**(5):634–642. doi:[10.1002/mds.870100517](https://doi.org/10.1002/mds.870100517)
- Ulfberg J, Nyström B, Carter N, Edling C. Prevalence of restless legs syndrome among men aged 18 to 64 years: an association with somatic disease and neuropsychiatric symptoms. *Mov Disord*. 2001;**16**(6):1159–1163. doi:[10.1002/mds.1209](https://doi.org/10.1002/mds.1209)
- Phillips B, Young T, Finn L, Asher K, Hening WA, Purvis C. Epidemiology of restless legs symptoms in adults. *Arch Intern Med*. 2000;**160**(14):2137–2141. doi:[10.1001/archinte.160.14.2137](https://doi.org/10.1001/archinte.160.14.2137)
- Ohayon MM, O'Hara R, Vitiello MV. Epidemiology of restless legs syndrome: a synthesis of the literature. *Sleep Med Rev*. 2012;**16**(4):283–295. doi:[10.1016/j.smrv.2011.05.002](https://doi.org/10.1016/j.smrv.2011.05.002)
- Rothdach AJ, Trenkwalder C, Haberstock J, Keil U, Berger K. Prevalence and risk factors of RLS in an elderly population: the MEMO study Memory and Morbidity in Augsburg Elderly. *Neurology*. 2000;**54**(5):1064–1068. doi:[10.1212/wnl.54.5.1064](https://doi.org/10.1212/wnl.54.5.1064)
- Schormair B, Zhao C, Bell S, et al.; 23andMe Research Team. Identification of novel risk loci for restless legs syndrome in genome-wide association studies in individuals of European ancestry: a meta-analysis. *Lancet Neurol*. 2017;**16**(11):898–907. doi:[10.1016/S1474-4422\(17\)30327-7](https://doi.org/10.1016/S1474-4422(17)30327-7)
- Desai AV, Cherkas LF, Spector TD, Williams AJ. Genetic influences in self-reported symptoms of obstructive sleep apnoea and restless legs: a twin study. *Twin Res*. 2004;**7**(6):589–595. doi:[10.1375/1369052042663841](https://doi.org/10.1375/1369052042663841)
- Lavigne GJ, Montplaisir JY. Restless legs syndrome and sleep bruxism: prevalence and association among Canadians. *Sleep*. 1994;**17**(8):739–743.
- Strang RR. The symptom of restless legs. *Med J Aust*. 1967;**1**(24):1211–1213. doi:[10.5694/j.1326-5377.1967.tb73929.x](https://doi.org/10.5694/j.1326-5377.1967.tb73929.x)
- Berger K, Luedemann J, Trenkwalder C, John U, Kessler C. Sex and the risk of restless legs syndrome in the general population. *Arch Intern Med*. 2004;**164**(2):196–202. doi:[10.1001/archinte.164.2.196](https://doi.org/10.1001/archinte.164.2.196)

12. Szentkiralyi A, Fendrich K, Hoffmann W, Happe S, Berger K. Incidence of restless legs syndrome in two population-based cohort studies in Germany. *Sleep Med.* 2011;**12**(9):815–820. doi:[10.1016/j.sleep.2011.06.016](https://doi.org/10.1016/j.sleep.2011.06.016)
13. Catoire H, Sarayloo F, Mourabit Amari K, et al. A direct interaction between two restless legs syndrome predisposing genes: MEIS1 and SKOR1. *Sci Rep.* 2018;**8**(1):12173. doi:[10.1038/s41598-018-30665-6](https://doi.org/10.1038/s41598-018-30665-6)
14. Winkelmann J, Schormair B, Lichtner P, et al. Genome-wide association study of restless legs syndrome identifies common variants in three genomic regions. *Nat Genet.* 2007;**39**(8):1000–1006. doi:[10.1038/ng2099](https://doi.org/10.1038/ng2099)
15. Cervenka S, Pålhaugen SE, Comley RA, et al. Support for dopaminergic hypoactivity in restless legs syndrome: a PET study on D2-receptor binding. *Brain.* 2006;**129**(Pt 8):2017–2028. doi:[10.1093/brain/awl163](https://doi.org/10.1093/brain/awl163)
16. Allen RP, Barker PB, Wehrl FW, Song HK, Earley CJ. MRI measurement of brain iron in patients with restless legs syndrome. *Neurology.* 2001;**56**(2):263–265. doi:[10.1212/wnl.56.2.263](https://doi.org/10.1212/wnl.56.2.263)
17. Salminen AV, Silvani A, Allen RP, et al.; International Restless Legs Syndrome Study Group (IRLSSG). Consensus guidelines on rodent models of restless legs syndrome. *Mov Disord.* 2021;**36**(3):558–569. doi:[10.1002/mds.28401](https://doi.org/10.1002/mds.28401)
18. Azcoitia V, Aracil M, Martínez-A C, Torres M. The homeodomain protein Meis1 is essential for definitive hematopoiesis and vascular patterning in the mouse embryo. *Dev Biol.* 2005;**280**(2):307–320. doi:[10.1016/j.ydbio.2005.01.004](https://doi.org/10.1016/j.ydbio.2005.01.004)
19. Salminen AV, Garrett L, Schormair B, et al.; German Mouse Clinic Consortium. Meis1: effects on motor phenotypes and the sensorimotor system in mice. *Dis Model Mech.* 2017;**10**(8):981–991. doi:[10.1242/dmm.030080](https://doi.org/10.1242/dmm.030080)
20. Lyu S, Xing H, Liu Y, et al. Deficiency of Meis1, a transcriptional regulator, in mice and worms: neurochemical and behavioral characterizations with implications in the restless legs syndrome. *J Neurochem.* 2020;**155**(5):522–537. doi:[10.1111/jnc.15177](https://doi.org/10.1111/jnc.15177)
21. Leon-Sarmiento FE, Peckham E, Leon-Ariza DS, Bara-Jimenez W, Hallett M. Auditory and lower limb tactile prepulse inhibition in primary restless legs syndrome: clues to its pathophysiology. *J Clin Neurophysiol.* 2015;**32**(4):369–374. doi:[10.1097/WNP.0000000000000196](https://doi.org/10.1097/WNP.0000000000000196)
22. Salminen AV, Schormair B, Flachskamm C, et al. Sleep disturbance by pramipexole is modified by Meis1 in mice. *J Sleep Res.* 2018;**27**(4):e12557. doi:[10.1111/jsr.12557](https://doi.org/10.1111/jsr.12557)
23. Salminen AV, Lam DD, Winkelmann J. Role of MEIS1 in restless legs syndrome: from GWAS to functional studies in mice. In: Stefan C and Imad G, eds. *Advances in Pharmacology*. Vol. **84**. Amsterdam: Elsevier; 2019: 175–184. doi:[10.1016/bs.apha.2019.03.003](https://doi.org/10.1016/bs.apha.2019.03.003)
24. Schulte EC, Kousi M, Tan PL, et al. Targeted resequencing and systematic in vivo functional testing identifies rare variants in MEIS1 as significant contributors to restless legs syndrome. *Am J Hum Genet.* 2014;**95**(1):85–95. doi:[10.1016/j.ajhg.2014.06.005](https://doi.org/10.1016/j.ajhg.2014.06.005)
25. Wefers B, Wurst W, Kühn R. Gene editing in mouse zygotes using the CRISPR/Cas9 system. In: Saunders TL, ed. *Transgenesis*. Vol. 2631. *Methods in Molecular Biology*. New York, NY: Springer US; 2023: 207–230. doi:[10.1007/978-1-0716-2990-1_8](https://doi.org/10.1007/978-1-0716-2990-1_8)
26. Fuchs H, Aguilar-Pimentel JA, Amarie OV, et al. Understanding gene functions and disease mechanisms: phenotyping pipelines in the German Mouse Clinic. *Behav Brain Res.* 2018;**352**:187–196. doi:[10.1016/j.bbr.2017.09.048](https://doi.org/10.1016/j.bbr.2017.09.048)
27. Gailus-Durner V, Fuchs H, Becker L, et al. Introducing the German Mouse Clinic: open access platform for standardized phenotyping. *Nat Methods.* 2005;**2**(6):403–404. doi:[10.1038/nmeth0605-403](https://doi.org/10.1038/nmeth0605-403)
28. Rozman J, Klingenspor M, Hrabě de Angelis M. A review of standardized metabolic phenotyping of animal models. *Mamm Genome.* 2014;**25**(9–10):497–507. doi:[10.1007/s00335-014-9532-0](https://doi.org/10.1007/s00335-014-9532-0)
29. Lusk G. Animal calorimetry. *J Biol Chem.* 1924;**59**(1):41–42. doi:[10.1016/s0021-9258\(18\)85293-0](https://doi.org/10.1016/s0021-9258(18)85293-0)
30. Nie Y, Gavin TP, Kuang S. Measurement of resting energy metabolism in mice using Oxymax open circuit indirect calorimeter. *Bio Protoc.* 2015;**5**(18):e1602. doi:[10.21769/bioprotoc.1602](https://doi.org/10.21769/bioprotoc.1602)
31. Bartolucci ML, Berteotti C, Alvente S, et al. Obstructive sleep apneas naturally occur in mice during REM sleep and are highly prevalent in a mouse model of Down syndrome. *Neurobiol Dis.* 2021;**159**:105508. doi:[10.1016/j.nbd.2021.105508](https://doi.org/10.1016/j.nbd.2021.105508)
32. Eddy NB, Leimbach D. Synthetic analgesics. II. Dithienylbutenyl- and dithienylbutylamines. *J Pharmacol Exp Ther.* 1953;**107**(3):385–393.
33. Mang GM, Nicod J, Emmenegger Y, Donohue KD, O'Hara BF, Franken P. Evaluation of a piezoelectric system as an alternative to electroencephalogram/electromyogram recordings in mouse sleep studies. *Sleep.* 2014;**37**(8):1383–1392. doi:[10.5665/sleep.3936](https://doi.org/10.5665/sleep.3936)
34. Rathkolb B, Hans W, Prehn C, et al. Clinical chemistry and other laboratory tests on mouse plasma or serum. *Curr Protoc Mouse Biol.* 2013;**3**(2):69–100. doi:[10.1002/9780470942390.mo130043](https://doi.org/10.1002/9780470942390.mo130043)
35. Zhang H, Zhang Y, Ren R, et al. Polysomnographic features of idiopathic restless legs syndrome: a systematic review and meta-analysis of 13 sleep parameters and 23 leg movement parameters. *J Clin Sleep Med.* 2022;**18**(11):2561–2575. doi:[10.5664/jcsm.10160](https://doi.org/10.5664/jcsm.10160)
36. DeAndrade MP, Johnson RL, Unger EL, et al. Motor restlessness, sleep disturbances, thermal sensory alterations and elevated serum iron levels in Btd9 mutant mice. *Hum Mol Genet.* 2012;**21**(18):3984–3992. doi:[10.1093/hmg/dds221](https://doi.org/10.1093/hmg/dds221)
37. Whittom S, Dauvilliers Y, Pennestri MH, et al. Age-at-onset in restless legs syndrome: a clinical and polysomnographic study. *Sleep Med.* 2007;**9**(1):54–59. doi:[10.1016/j.sleep.2007.01.017](https://doi.org/10.1016/j.sleep.2007.01.017)
38. Trenkwalder C, Paulus W. Restless legs syndrome: pathophysiology, clinical presentation and management. *Nat Rev Neurol.* 2010;**6**(6):337–346. doi:[10.1038/nrneurol.2010.55](https://doi.org/10.1038/nrneurol.2010.55)
39. Xie K, Fuchs H, Scifo E, et al. Deep phenotyping and lifetime trajectories reveal limited effects of longevity regulators on the aging process in C57BL/6J mice. *Nat Commun.* 2022;**13**(1):6830. doi:[10.1038/s41467-022-34515-y](https://doi.org/10.1038/s41467-022-34515-y)
40. Silva GE, Goodwin JL, Vana KD, Vasquez MM, Wilcox PG, Quan SF. Restless legs syndrome, sleep, and quality of life among adolescents and young adults. *J Clin Sleep Med.* 2014;**10**(7):779–786. doi:[10.5664/jcsm.3872](https://doi.org/10.5664/jcsm.3872)
41. Schattschneider J, Bode A, Wasner G, Binder A, Deuschl G, Baron R. Idiopathic restless legs syndrome: abnormalities in central somatosensory processing. *J Neurol.* 2004;**251**(8):977–982. doi:[10.1007/s00415-004-0475-3](https://doi.org/10.1007/s00415-004-0475-3)
42. Bachmann CG, Rolke R, Scheidt U, et al. Thermal hypoaesthesia differentiates secondary restless legs syndrome associated with small fibre neuropathy from primary restless legs syndrome. *Brain.* 2010;**133**(3):762–770. doi:[10.1093/brain/awq026](https://doi.org/10.1093/brain/awq026)
43. Happe S, Zeitlhofer J. Abnormal cutaneous thermal thresholds in patients with restless legs syndrome. *J Neurol.* 2003;**250**(3):362–365. doi:[10.1007/s00415-003-0987-2](https://doi.org/10.1007/s00415-003-0987-2)
44. Winkelmann JW, Gagnon A, Clair AG. Sensory symptoms in restless legs syndrome: the enigma of pain. *Sleep Med.* 2013;**14**(10):934–942. doi:[10.1016/j.sleep.2013.05.017](https://doi.org/10.1016/j.sleep.2013.05.017)
45. Woods S, Basco J, Clemens S. Effects of iron-deficient diet on sleep onset and spinal reflexes in a rodent model of restless legs syndrome. *Front Neurol.* 2023;**14**:1160028. doi:[10.3389/fneur.2023.1160028](https://doi.org/10.3389/fneur.2023.1160028)
46. Sarberg M, Josefsson A, Wiréhn A, Svanborg E. Restless legs syndrome during and after pregnancy and its relation to snoring. *Acta Obstet Gynecol Scand.* 2012;**91**(7):850–855. doi:[10.1111/j.1600-0412.2012.01404.x](https://doi.org/10.1111/j.1600-0412.2012.01404.x)